

Collective excitation of ^{172}Yb from inelastic α scattering at 36 MeV

I. M. Govil,* H. W. Fulbright, and D. Cline

Nuclear Structure Research Laboratory, University of Rochester, Rochester, New York 14627

(Received 8 June 1987)

The collective excitation of the natural parity states in ^{172}Yb has been studied with 36 MeV α particles. An analysis of the ground-state band data through $I^\pi=6^+$ gave deformation parameters $\beta_2=+0.21\pm 0.01$, $\beta_4=-0.028\pm 0.004$, and $\beta_6=0\pm 0.002$. Two $K^\pi=2^+$ bands, with band heads at 1465 and 1608 keV, and the β vibrational $K^\pi=0^+$ band with a 2^+ state at 1118 keV are excited weakly. Other 2^+ states at 2184, 2255, 2367, 2465, 2580, 2650, 2738, 2836, 2890, and 2955 keV are seen, and their isoscalar strengths are found for the first time. The $B(E2)$ strengths found are roughly in agreement with interacting boson model predictions close to the SU(3) limit. At 1263 keV, the 4^+ state of the $K^\pi=3^+$ band is found to have an isoscalar $E4$ strength $=0.036 e^2b^4$ (7 single particle units). A compilation plus reanalysis of earlier data exhibits unexpectedly strong $E4$ strength to the 4^+ members of the lowest $K=2^+$ and 3^+ bands in strongly deformed rare earth nuclei. The octupole strength in this nucleus lies mainly in four 3^- states at 1222, 1710, 1822, and 2030 keV with total isoscalar $E3$ strength of $0.147 e^2b^3$. The results for the negative parity states are compared with the theory of Neergård and Vogel.

I. INTRODUCTION

The energy spectrum of ^{172}Yb is known from radioactive decay,^{1,2} and from $(\alpha, 2n)$ ^{3,4} and (n, γ) ⁵⁻⁷ experiments. The ground-state band of this nucleus has a well deformed rotational structure⁸ in conformity with its immediate neighbors, yet in some features it differs from adjacent nuclei. The γ vibration in this nucleus occurs at higher excitation energy than the β vibration in contrast to ^{168}Er . Inelastic (d, d') and single particle transfer studies by Burke and Elbek,⁹ using 12 MeV deuterons, have shown evidence that the 2^+ state at 1468 keV is the first member of the $K^\pi=2^+$ γ vibrational band. On the other hand, on the basis of microscopic calculations, Soloviev¹⁰ has suggested that this state is primarily of $\frac{1}{2}[521]-\frac{5}{2}[512]$, $K=2$, two-quasineutron character. Also there has been debate on the collectivity of excited 0^+ β vibrational bands, since these bands are excited strongly in two neutron transfer reactions.¹¹ The reduction in the $B(E2)$ values between the γ and ground-state bands and also between the β and ground-state bands in this nucleus, relative to neighboring nuclei, has been attributed by Casten *et al.*¹² to the onset of an SU(3) symmetry within the interacting boson approximation (IBA) model. Coulomb excitation studies¹³⁻¹⁵ have provided $B(E1)$ values for low lying 2^+ and 3^- states but these values differ considerably among themselves and also from the results of inelastic scattering of 12 MeV deuterons by Burke and Elbek.⁹ The negative-parity $K^\pi=1^-$ octupole band¹⁶ is reported to be strongly perturbed by Coriolis coupling with the $K^\pi=0^-$ octupole band, which results in a significant odd-even shift in the rotational spacing of the $K^\pi=1^-$ band. The present study exploits the selectivity of inelastic alpha scattering in order to study the collective behavior of 2^+ , 4^+ , and 3^- states.

II. EXPERIMENTAL DETAILS

The experiment was done with 36 MeV α particles from the tandem Van de Graaff accelerator at the Nuclear Structure Research Laboratory of the University of Rochester. The experimental method is described in earlier papers.^{17,18} The targets in this case were 100–200 $\mu\text{g}/\text{cm}^2$ of 97% enrichment ^{172}Yb evaporated onto 20 $\mu\text{g}/\text{cm}^2$ carbon foils. During evaporation thorium metal was used to reduce enriched Yb_2O_3 obtained from Oak Ridge National Laboratory. The scattered α particle spectrum was obtained using an Enge split-pole spectrometer in conjunction with a position-sensitive delay-line-readout proportional counter in the focal plane. The overall energy resolution for α particles was better than 18 keV. The beam alignment was adjusted carefully to minimize slit scattering. The α spectrum was recorded at scattering angles from 15° to 75° at intervals of 2.5° . At angles $\leq 30^\circ$ a 1-mm-wide slit was used at the entrance to the spectrometer to reduce the widths of the kinematically broadened elastic background peaks of light element impurities. A solid state monitor detector placed at 45° provided relative normalization. Absolute cross sections were determined from Rutherford scattering at forward angles.

A spectrum of the α particles 55° is shown in Fig. 1. The centroids of the peaks were located with an accuracy of ± 5 keV. Figure 2 shows the energy level diagram proposed by Gelletly *et al.*⁵ on the basis of (n, γ) studies. The thick solid lines represent the states observed in the present experiment. The excited natural-parity states include all members of the ground-state band through 8^+ , the 0^+ and 2^+ states of the β vibrational band with the 0_2^+ band head at 1042 keV, 2^+ states at 1466 and 1608 keV corresponding to two $K=2^+$ bands, the 4^+ states at 1263 and 1658 keV belonging to $K=3^+$ band head at 1172 keV, and the $K=2^+$ band head at 1466 keV, re-

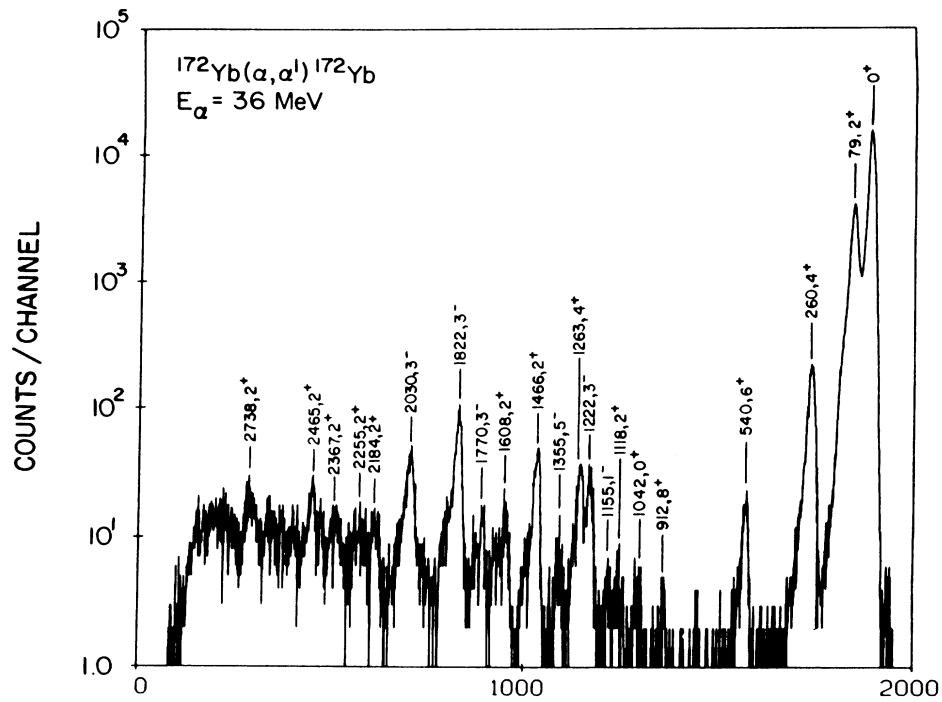
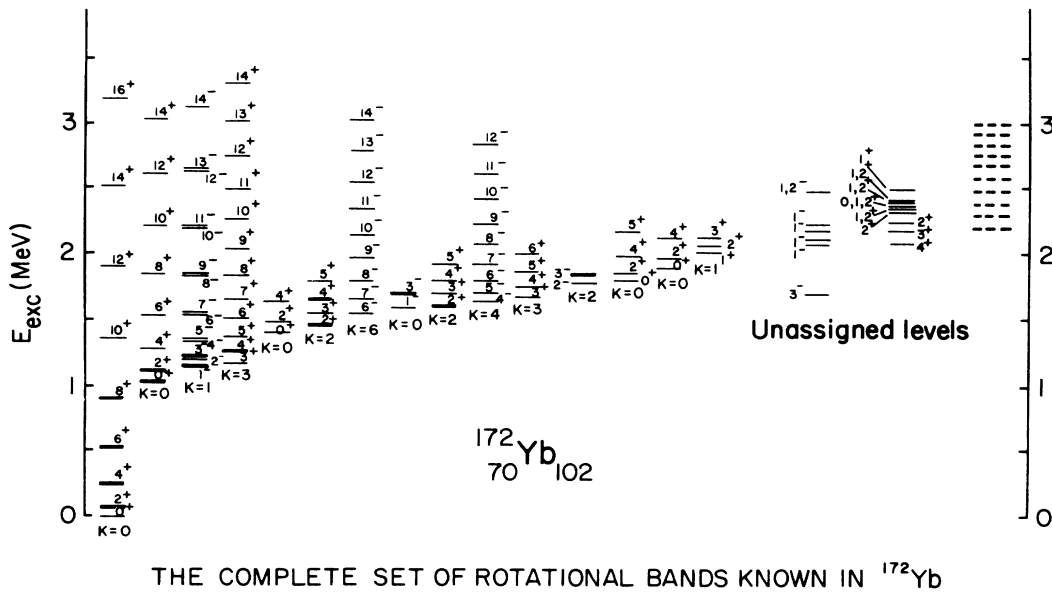


FIG. 1. Spectrum of scattered α particles at 55° .

spectively. The negative-parity states seen include 1^- (1155 keV), 3^- (1222 keV), and 5^- (1355 keV) members of the $K=1^-$ band, a 3^- state at 1710 keV corresponding to a $K=0^-$ band that has the 1^- band head at 1599 keV, a 3^- state at 1822 keV belonging to a $K=2^-$ band head at 1757 keV, and a 3^- state at 2030

keV corresponding to a $K=3^-$ band. A number of other states of unknown spin were excited at 2184, 2255, 2367, 2465, and 2738 keV. There is evidence of peaks at 2580, 2650, 2836, 2890, and 2995 keV but these energies are uncertain to 5 keV or more because of poor statistics.



THE COMPLETE SET OF ROTATIONAL BANDS KNOWN IN ^{172}Yb

FIG. 2. Energy level diagram proposed by Gelletly *et al.* (Ref. 5) from the (n,γ) resonance measurement. The levels excited in the present experiment are represented by thick solid lines and thick broken lines (newly excited).

III. ANALYSIS

A. Ground state band

Analysis of the ground-band data was made by use of the coupled channel code ECIS79 of Raynal¹⁹ in the framework of the rotational model. The complex optical model potential in the body fixed frame of reference has a Woods-Saxon form with volume absorption to which the Coulomb potential is added, i.e.,

$$V(r, \theta', \phi') = -(V + iW)(i + e)^{-1} + V_{\text{Coul}} \quad (3.1)$$

with

$$e = \exp\{[r - R(\theta', \phi')]/a\} \quad (3.2)$$

and

$$R(\theta', \phi') = R_0(1 + \beta_2 Y'_{20} + \beta_4 Y'_{40} + \beta_6 Y'_{60}) . \quad (3.3)$$

The optical potential parameters V (64.28 MeV), W (29.44 MeV), R_0 ($1.52 A^{1/3}$ fm), a_V (0.567 fm), and a_W (0.397 fm) were obtained by an automatic search feature of ECIS79 for the best fit of the elastic scattering data with inclusion of the first 2^+ state in the calculations.²⁰ For simplicity, the radius and the deformation parameters for each potential were held constant. The 4^+ state then was introduced and a search was made on β_2 and β_4 simultaneously and so on for the 6^+ state. During the search of the coupled channels the normalization factor for the elastic scattering cross section was readjusted.

$$\bar{v}_{\lambda K}^{(2)}(r) = \sum_{l=0,2,4} \beta_{3K} v_l^{(2)}(r) \left[\frac{7(2l+1)}{4\pi(2\lambda+1)} \right]^{1/2} [\langle 1030 | \lambda 0 \rangle \langle 103K | \lambda K \rangle - \xi_\mu \langle 1010 | \lambda 0 \rangle \langle 101K | \lambda K \rangle] . \quad (3.6)$$

The second term within the square brackets is the correction term for spurious center of mass motion.²² However, ξ_μ is not an independent variable but it is given in terms of β_{3K} by the translational invariance condition

$$\int \bar{v}_{\lambda=1}^{(2)}(r) r^3 dr = 0 .$$

C. Excited $K=0^+$, 2^+ , 3^+ , and 4^+ bands

The form factors for the β and γ vibrational bands built on a permanent quadrupole deformation were de-

$$\bar{v}_{\lambda k}^{(2)}(r) = \sum_{l=0,2,4} \beta_{\alpha K} v_l^{(2)}(r) \left[\frac{(2\alpha+1)(2l+1)}{4\pi(2\lambda+1)} \right]^{1/2} [\langle 10\alpha 0 | \lambda 0 \rangle \langle 10\lambda K | \lambda K \rangle - \xi_\beta \langle 1000 | \lambda 0 \rangle \langle 100K \lambda K \rangle] . \quad (3.8)$$

The correction term in this case is added to satisfy the condition for the conservation of volume; ξ_β is derived in terms of $\beta_{\alpha K}$ via the equation²³

$$\int V_{\lambda=0}^{(2)}(r) r^2 dr = 0 . \quad (3.9)$$

The static deformation parameter β_2 for the ground state band and β or γ vibrational bands are assumed to be the same in the present calculations.

B. Octupole vibrational band

The analysis of 3^- octupole states was done in the framework of a model of octupole vibration of an axially symmetric and statically deformed nucleus with the radius parameter given by

$$R(\theta', \phi') = R_0(1 + \beta_2 Y'_{20} + \beta_4 Y'_{40} + \beta_{3K} Y'_{3K}) . \quad (3.4)$$

Since ECIS79 does not have any built-in provision for treating such a case, the form factors connecting the states of the ground-state band to the octupole vibration band were derived using the prescription of Tamura²¹ and as described earlier¹⁸ for ^{168}Er . The final form of the optical potential used in the present coupled channel calculations is given by

$$V(r, \theta, \phi) = \sum_{l\mu} v_l^{(1)} D_{\mu 0}^l Y_{l\mu}(\theta, \phi) + \sum_{\lambda\mu} \bar{v}_{\lambda K}^{(2)}(r) D_{\mu K}^\lambda Y_{\lambda\mu} . \quad (3.5)$$

The first term connects the states of the same rotational band, while the second term connects the ground-state band to the members of other rotational bands built on the octupole vibrational states $K=0, 1, 2, 3$, etc.

The form factors $v_l^{(1)}$ for the first term were calculated internally by the program while the form factors for the second term were calculated externally and fed to ECIS79. These form factors are given by

rived in a way similar to those described for the 3^- states, with the radius parameter given in the body frame of reference by

$$R(\theta', \phi') = R_0(1 + \beta_2 Y'_{20} + \beta_4 Y'_{40} + \sum_{\alpha K} \beta_{\alpha K} Y'_{\alpha K}) . \quad (3.7)$$

The β_2 and β_4 are the static deformations and $\beta_{\alpha K}$ represents the vibrational amplitude of $\alpha=2$ (quadrupole) or $\alpha=4$ (hexadecupole) vibration for $k=2^+, 3^+$, or 4^+ bands. The form factors connecting the states of the ground state band to the states of excited $K=2^+, 3^+$, and 4^+ bands are calculated externally, which are given by

IV. RESULTS AND DISCUSSION

A. Ground state band

Figure 3 shows the results of the coupled channel calculations for the ground state band and the experimental cross sections. The following values of the deformation parameters,

$$\begin{aligned}\beta_2 &= 0.21 \pm 0.01, \\ \beta_4 &= -0.028 \pm 0.004, \\ \beta_6 &= 0.0 \pm 0.002,\end{aligned}$$

were obtained by minimizing χ^2 with all the members of the ground-state band through 8^+ included in the calculations.

B. Quadrupole vibrational states

The measured and calculated cross sections for the β vibrational 2^+ state at 1118 keV and γ vibrational 2^+ states at 1466 and 1608 keV are shown in Fig. 4. The 1118 keV 2^+ $K=0^+$ state is weakly excited and its cross section could be measured only at a few angles. This weak excitation is consistent with the two-quasiparticle configuration suggested by Soloviev.¹⁰ The γ vibrational state at 1466 keV has $\beta_{22}=0.014$. The ratio between de-

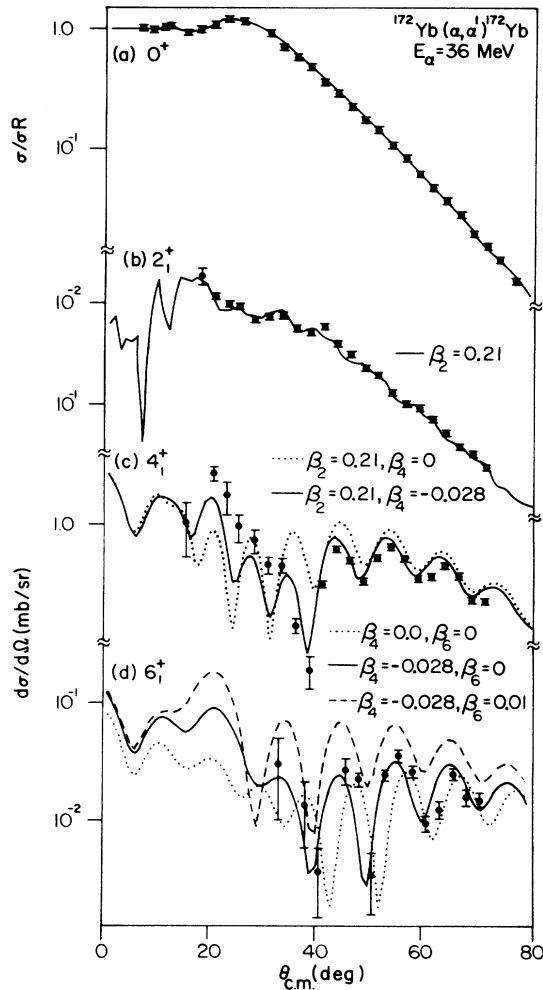


FIG. 3. Experimental data and symmetric rotor model coupled channel results for (α, α') reactions at $E_\alpha = 36$ MeV; (a) 0^+ g.s.; (b) 2_1^+ (79 keV) state; (c) 4_1^+ (260 keV) state; and (d) 6_1^+ (540 keV) state.

formation parameters β_{22} ($\beta_2 \sin \gamma$) for the γ band and β_{20} ($\beta_2 \cos \gamma = 0.21$) for the 2^+ state of the ground-state band gives a $\langle \gamma \rangle$ value $= 3.9^\circ$, representative of weak collective γ vibration as compared to its neighbor ^{168}Er for which $\gamma = 9^\circ$. The $\beta_{22} = 0.0074$ for the 1608 keV state represents even weaker collective γ character, consistent with the particle transfer (d,t) data,^{9,16} indicating that this state contains a large fraction of $[\frac{5}{2}^-[512], \frac{1}{2}^-[521]]$ two-neutron configuration.

Table I shows the $B(E1, 0 \rightarrow 1)$ isoscalar transition strengths for positive parity states obtained in the present experiment. The isoscalar transition strengths are derived from the deformation parameters by exploiting the formal similarity between electromagnetic and inelastic transition strengths outlined by Bernstein²⁴ and using the Satchler theorem²⁵ described earlier.^{17,18} The values of the present isoscalar transition strengths are compared with the results of Coulomb excitation measurements. The $B(E2)$ value for the first excited 2^+ state of the ground state band is about 24% higher than the value obtained from Coulomb excitation by Wollersheim.¹⁴ The $B(E2)$ values for the 1466 and 1608 keV states of the γ vibrational band are close to the values obtained by Cresswell *et al.*⁴ but for the 1118 keV 2^+ state the Coulomb excitation value is about 5 times higher than our value.

The $B(E2)$ values for the 2^+ states at 2184, 2255,

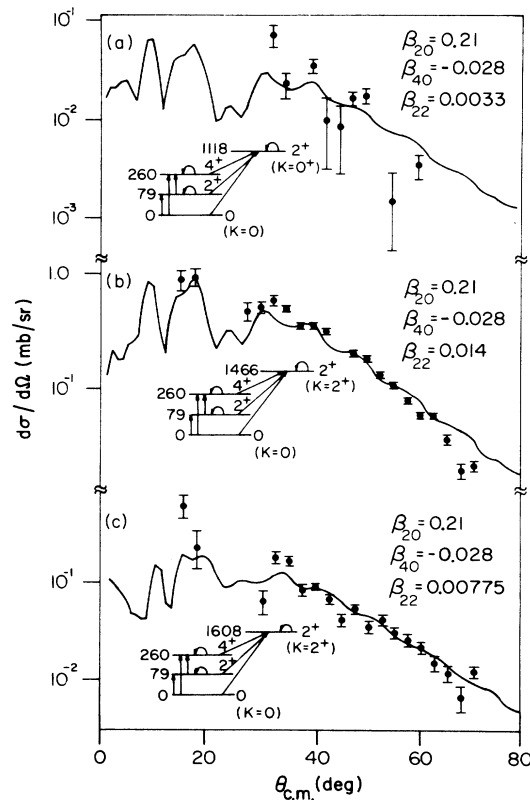


FIG. 4. Experimental data and the coupled channel results for (a) 2_2^+ (1118 keV, $K=0^+$) state; (b) 2_3^+ (1466 keV, $K=2^+$) state; (c) 2_4^+ (1608 keV, $K=2^+$) state.

2367, 2465, 2580, 2650, 2758, 2836, 2890, and 2995 keV are newly assigned. Because of weak excitation of these states it is difficult to make unique spin assignments. However, as shown in Fig. 5, 2^+ spin assignments seem more consistent with the data than 3^- for most of these states. On the basis of (p,t) results, the levels at 2184 and 2254 keV were tentatively assigned 2^+ by Oothoudt and Hintz,¹¹ who also identified levels at 2364, 2460, 2580, 2734, and 2832 keV but made no spin assignment. These levels may be compared with those seen in the present work at 2367, 2465, 2580, 2738, and 2836 keV.

In Table I the results are compared with the IBA model calculations using a Hamiltonian close to the SU(3) limit, i.e.,

$$H = 0.00867(L \cdot L) - 0.02125(Q \cdot Q) - 0.2645[(d^\dagger \tilde{d})^{(3)} \times (d^\dagger \tilde{d})^{(3)}]^0, \quad (4.1)$$

where the operators $(L \cdot L)$ and $(Q \cdot Q)$, etc. are as

defined by Schölten.²⁶ In a pure SU(3) limit the β and γ bands are degenerate; therefore the third term in square brackets is needed to raise the γ band above the β band.

The $B(E2)$ values were derived using the IBA model $E2$ transition operator:

$$T(E2) = E2SD(s^\dagger \tilde{d} + d^\dagger \tilde{s})^2 + 1/\sqrt{5}E2DD(d^\dagger d)^2. \quad (4.2)$$

For $E2DD/E2SD = -2.0$ there is a close agreement with IBA values for the first six transitions (up to 2255 keV), except for the 1608 keV state, where the experimental value is ≈ 50 times larger than the IBA value.

C. Octupole vibrational states

Figure 6 compares the coupled channel cross sections with data for the 3^- states. The form factors were calculated externally using Eq. (3.6) and fed to ECIS79 to calculate the cross sections. The couplings involved in the calculations are shown in the inset for each state.

TABLE I. Comparison of the present isoscalar transition strengths for positive parity states with the isoscalar (d,d') strengths, Coulomb excitation measurements, and IBA predictions.

| Transition $I_i \rightarrow I_f(K)$ | Energy (keV) | El | Present results | | (d,d') $B(IS)^b$ (e^2b') | Coulomb excitation $B(EM)$ (e^2b') | IBA Theory $B(IBA)$ (e^2b') |
|----------------------------------------|-----------------|------|---------------------|---------------------------------|------------------------------------|--------------------------------------------------------------------------|------------------------------------------|
| | | | $B(IS)$ (s.p.u.) | $B(IS)^a$ (e^2b') | | | |
| $0^+ \rightarrow 2_1^+(0)$ | 79 | $E2$ | 265 | 7.5(9) | 7.55 | 6.04(6) ^c 5.95(48) ^d | 7.5 ^g |
| $0^+ \rightarrow 2_2^+(0)$ | 1118 | $E2$ | 0.05 | 0.0015(5) | 0.0026 | 0.0068(5) ^d 0.0066(3) ^e 0.035 ^f | 0.0062 |
| $0^+ \rightarrow 2_3^+(2)$ | 1466 | $E2$ | 1.4 | 0.041(9) | 0.041 | 0.0373(29) ^d 0.0395(16) ^e 0.186 ^f | 0.030 |
| $0^+ \rightarrow 2_4^+(2)$ | 1608 | $E2$ | 0.42 | 0.012(3) | 0.0053 | 0.0159(17) ^d 0.0101(7) ^e | 0.0002 |
| $0^+ \rightarrow 2_5^+$ | 2184 | $E2$ | 0.07 | 0.0019(4) | | | 0.00028 |
| $0^+ \rightarrow 2_6^+$ | 2255 | $E2$ | 0.1 | 0.0029(6) | | | 0.0058 |
| $0^+ \rightarrow 2_7^+$ | 2367 | $E2$ | 0.18 | 0.005(1) | | | 0.0009 |
| $0^+ \rightarrow 2_8^+$ | 2465 | $E2$ | 0.35 | 0.010(2) | | | 0.0 |
| $0^+ \rightarrow 2_9^+$ | 2580 | $E2$ | 0.12 | 0.0034(7) | | | |
| $0^+ \rightarrow 2_{10}^+$ | 2650 | $E2$ | 0.13 | 0.0038(8) | | | |
| $0^+ \rightarrow 2_{11}^+$ | 2738 | $E2$ | 0.42 | 0.012(3) | | | |
| $0^+ \rightarrow 2_{12}^+$ | 2836 | $E2$ | 0.25 | 0.0072(15) | | | |
| $0^+ \rightarrow 2_{13}^+$ | 2890 | $E2$ | 0.6 | 0.017(4) | | | |
| $0^+ \rightarrow 2_{14}^+$ | 2995 | $E2$ | 0.3 | 0.0087(17) | | | |
| $0^+ \rightarrow 4_1^+(0)$ | 260 | $E4$ | 0.05 | 0.0003(± 97) ^h | | 0.044(± 80) ^c | |
| $0^+ \rightarrow 4_3^+(3)$ | 1263 | $E4$ | 6.9 | 0.036(7) | | | |
| $0^+ \rightarrow 4_5^+(2)$ | 1658 | $E4$ | 1.1 | 0.006(2) | | | |
| $0^+ \rightarrow 4_6^+(2)$ | 1803 | $E4$ | ≤ 2.2 | ≤ 0.012 | | | |
| $0^+ \rightarrow 6_1^+(0)$ | 540 | $E6$ | 4.1 | 0.004(± 82) ^h | | | |

^aThe errors shown in the parentheses include only the statistical error and do not include any systematic error due to model, cross correlations in deformation parameters, or reaction mechanism dependence.

^bReference 9. The authors have calculated $B(E2)$ from the relation $B(E2) = 1.18(d\sigma/d\Omega)_{90^\circ}$.

^cReference 14.

^dReference 13.

^eReference 4.

^fReference 15.

^gThis value is used to normalize the results of the IBA calculations.

^hThe matrix elements for these transitions are negative assuming positive in-band $E2$ transition matrix elements.

The dip in the experimental cross sections at $\theta \approx 30^\circ$ is nicely reproduced for the 2030 and 1822 keV states. Few data points for the 1222 and 1710 keV states could be obtained at small angles because of carbon and oxygen impurity scattering. The sensitivity of the calculated cross sections to parameter variation is shown in Fig. 7. Changing the Coulomb radius [Fig. 7(b)], changing the K value of the band [Fig. 7(c)], and assuming a β_2 value for the 3^- state band different from the ground-band value [Fig. 7(d)] have minor effects on the angular distributions. However, the calculated cross sections show sensitivity to the quadrupole moment of the 3^- states [Fig. 7(a)], which were assumed to be given by the rotational model.

In Table II the present isoscalar $B(E3)$ values and the Coulomb excitation values are given along with the Neergård and Vogel²⁷ predictions. Our values are in better agreement with the (d,d') results⁹ than the values obtained by Cresswell.⁴ The predictions from Neergård and Vogel's calculations (random phase approximation) agree fairly well only for the transition strength to the 3^- state at 1822 keV ($K=2^-$), while the theory overestimates, by a factor of 3.5, excitation of the 1710 keV ($K=0^-$) state and underestimates, by an order of mag-

nitude, for the 2030 keV state ($K=3^-$). The total isoscalar sum $B(E3)$ strength ($BE3,0 \rightarrow 3^-$) observed in this nucleus in $0.147 e^2 b^3$ with an energy centroid at 1832 keV, which can be compared with the total sum $B(E3,0 \rightarrow 3)$ strength $= 0.235 e^2 b^3$, with centroid at 1907 keV,²⁸ found for ^{168}Er and the value

$$B(E3,0 \rightarrow 3) = 0.33 \pm 0.04 e^2 b^3$$

for the single 3^- state²⁹ at 1579 keV in the nearby doubly closed shell nucleus ^{146}Gd .

D. Hexadecupole vibrational states

In contrast to the weak excitation of the ground band 4^+ state (0.05 s.p.u.), a comparatively strong excitation (6.3 s.p.u) to the 4^+ state of the $K=3^+$ band was observed in the present experiment. The β_{43} value for this state has been obtained with the form factor given by Eq. (3.8) and the angular distribution shown in Fig. 8.

Figure 9 summarizes experimental $E4$ matrix elements³⁰⁻⁴⁵ coupling the ground state to the 4^+ states of the $K=0^+, 2^+, 3^+$, and 4^+ bands, in the strongly deformed rare earth nuclei ($150 < A < 200$). The systematics of the $E4$ matrix elements between the 0^+ and the 4^+ states of the $K=0$ ground band is well known. The

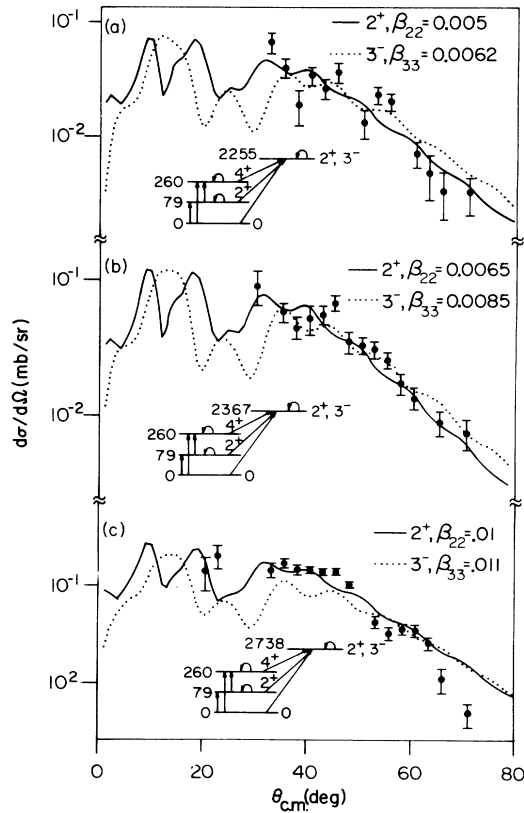


FIG. 5. Experimental data and the coupled channel results in the framework of octupole (dotted curve) and quadrupole (solid curve) vibration of an axially symmetric and statically deformed nucleus with $\beta_2 = 0.21$ for (a) 2255 keV state; (b) 2367 keV state; (c) 2738 keV state.

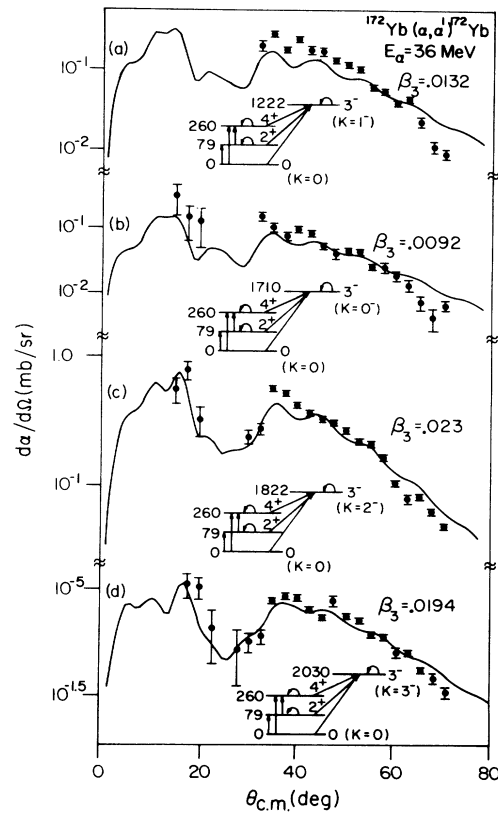


FIG. 6. Experimental data and coupled channel results for the 3^- states (a) 3^- (1222 keV, $K=1^-$) state; (b) 3^- (1710 keV, $K=0^-$) state; (c) 3^- (1822 keV, $K=2^-$) state; (d) 3^- (2030 keV, $K=3^-$) state.

small $B(E4)$ values obtained for the ground state $K=0$ band in ^{172}Yb from the present measurement and for ^{168}Er , from our earlier measurement,¹⁸ are consistent with the systematics and the known change in sign at

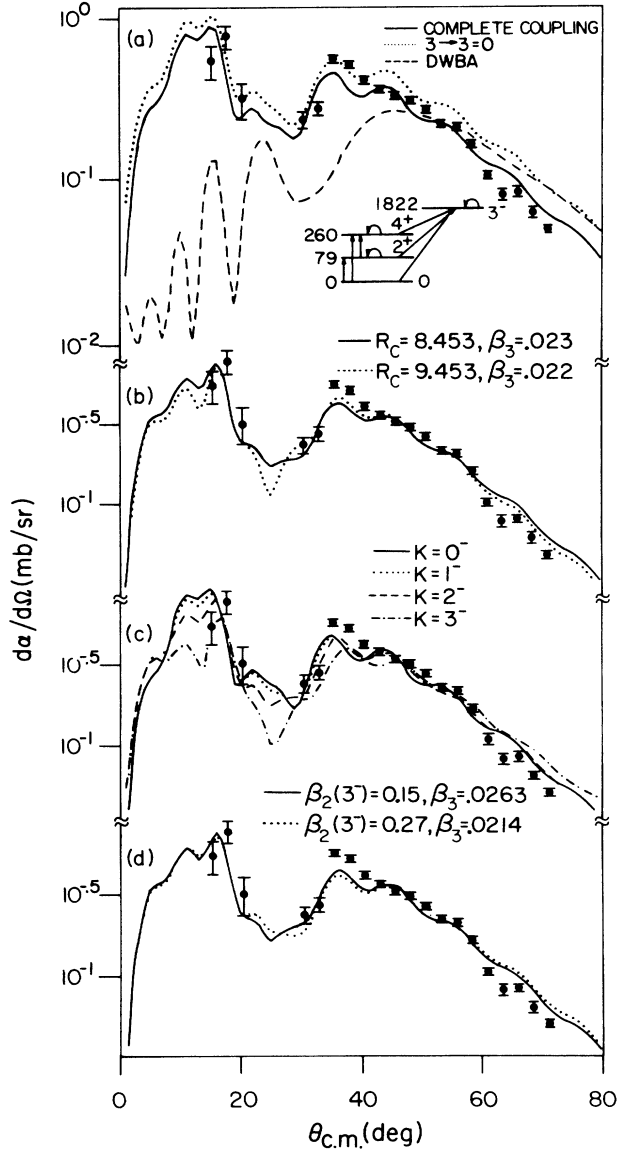


FIG. 7. Experimental data and the effect of the various couplings and potential parameters for the 1822 keV 3^- state; (a) the complete coupling as shown in the inset of the diagram (solid curve), $3^- \rightarrow 3^-$ coupling (reorientation or quadrupole moment) has been set to zero (dotted curve) and one step DWBA prediction (dashed curve); (b) the effect of the Coulomb radius when $R_c = 8.453$ fm (solid curve) and $R_c = 9.453$ fm (dotted curve); (c) the effect of the variations of the K value of the band, $K=0$ (solid curve), $K=1$ (dotted curve), $K=2$ (dashed curve), and $K=3$ (dot-dashed curve); (d) the effect of the quadrupole deformation of the $K=2^-$ band belonging to the 1822 keV 3^- state, $\beta_2(K=2^-) = 0.15$, which is lower than the β_2 value (0.21) of the ground state band (solid curve), $\beta_2(K=2^-) = 0.27$, which is higher than the β_2 value of the g.s. band (dotted curve).

$A = 176$.

Prior to the present work, data on the $E4$ matrix elements coupling the ground state to the 4^+ states of the lowest $K=2^+$, 3^+ , and 4^+ bands were sparse. The present work determined the magnitudes and signs of the $E4$ matrix elements to the $K=2^+$ band and 3^+ bands to be positive in ^{172}Yb ; a positive value for the $K=2^+$ matrix element in ^{168}Er was obtained earlier.¹⁸ The relative phases of the wave functions are defined by assuming that the signs of the appropriate transition $E2$ matrix elements are positive. An earlier inelastic alpha scattering experiment by Todd Baker *et al.*⁴³ has suggested that the $E4$ matrix element to the $K=2^+$ band in ^{192}Os is positive while for the $K=4^+$ band it is either positive or negative. In the present work, $E4$ matrix elements were extracted from earlier inelastic deuteron scattering data³⁸⁻⁴² via distorted-wave Born approximation (DWBA) calculations, using the global optical model parameters of Daehnick *et al.*,⁴⁶ and the more extensive spin assignments now available. Interference with multistep $E2$ excitation was neglected; even though in some cases these effects are estimated³⁴ to be unimportant, the results of this analysis should be treated with caution. The sign of the $E4$ matrix element to the $K=2^+$, 3^+ , and 4^+ bands could not be determined by this simple analysis since interference effects were not included. Consequently only the magnitudes of the matrix elements to the $K=2^+$, 3^+ , and 4^+ bands are shown in Fig. 9. After completion of the present work we have noted that the $B(E4)$ values for the $K=2^+$ band for a few nuclei obtained recently⁴⁷ by Ichihara *et al.* agree fairly well with the values obtained in the present compilation.

The $E4$ matrix elements to the $K=2^+$ γ band show a strong dependence on nuclear species, peaking for ^{168}Er and then dropping dramatically at ^{172}Yb : the $B(E4)$ is 16.5 s.p.u. in ^{168}Er and only 1.1 s.p.u. in ^{172}Yb . The $E4$ matrix elements to the $K=3^+$ band are unexpectedly strong in ^{172}Yb and ^{168}Er : i.e., the $B(E4)$ values in ^{172}Yb and ^{168}Er are 6.9 and 3.5 s.p.u., respectively. The strong excitation to this band is not understood. It

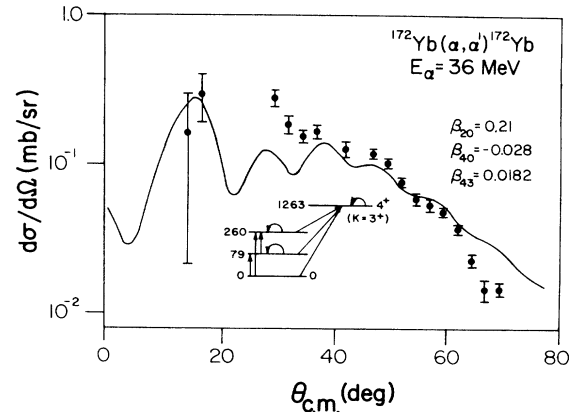


FIG. 8. Experimental data and the coupled channel results for the 1263 keV 4^+ state of the $K=3^+$ band.

TABLE II. Comparison of the present isoscalar transition strength for negative parity states with the isoscalar (d,d') strengths, Coulomb excitation results, and Neergård and Vogel predictions.

| Transition $I_i \rightarrow I_f (K)$ | Energy (keV) | El | Present results | | | Coulomb excitation $B(EM)^c$ (e^2b^l) | Neergård-Vogel (theory) (e^2b^l) | |
|-----------------------------------------|-----------------|------|---------------------|---------------------------|-------------------------------------|----------------------------------------------------|--------------------------------------------|-----------------|
| | | | $B(IS)$ (s.p.u.) | $B(IS)^a$ (e^2b^l) | (d,d') $B(IS)^b$ (e^2b^l) | | RPA ^d | CC ^e |
| $0 \rightarrow 3^-(1^-)$ | 1222 | $E3$ | 1.3 | 0.016(3) | 0.026 | 0.045 | 0.016 | 0.06 |
| $0 \rightarrow 3^-(0^-)$ | 1710 | $E3$ | 0.63 | 0.0078(16) | 0.015 | 0.025 | 0.027 | 0.026 |
| $0 \rightarrow 3^-(2^-)$ | 1822 | $E3$ | 5.2 | 0.065(13) | 0.053 | 0.033 | 0.048 | 0.017 |
| $0 \rightarrow 3^-(3^-)$ | 2030 | $E3$ | 4.7 | 0.058(12) | 0.022 | | 0.001 | 0.001 |

^aThe errors shown in the parentheses include only the statistical error and do not include any systematic error due to model dependence.

^bReference 9.

^cReference 4.

^dReference 27. Random phase approximation (RPA).

^eReference 27. Random phase approximation perturbed with Coriolis coupling (CC).

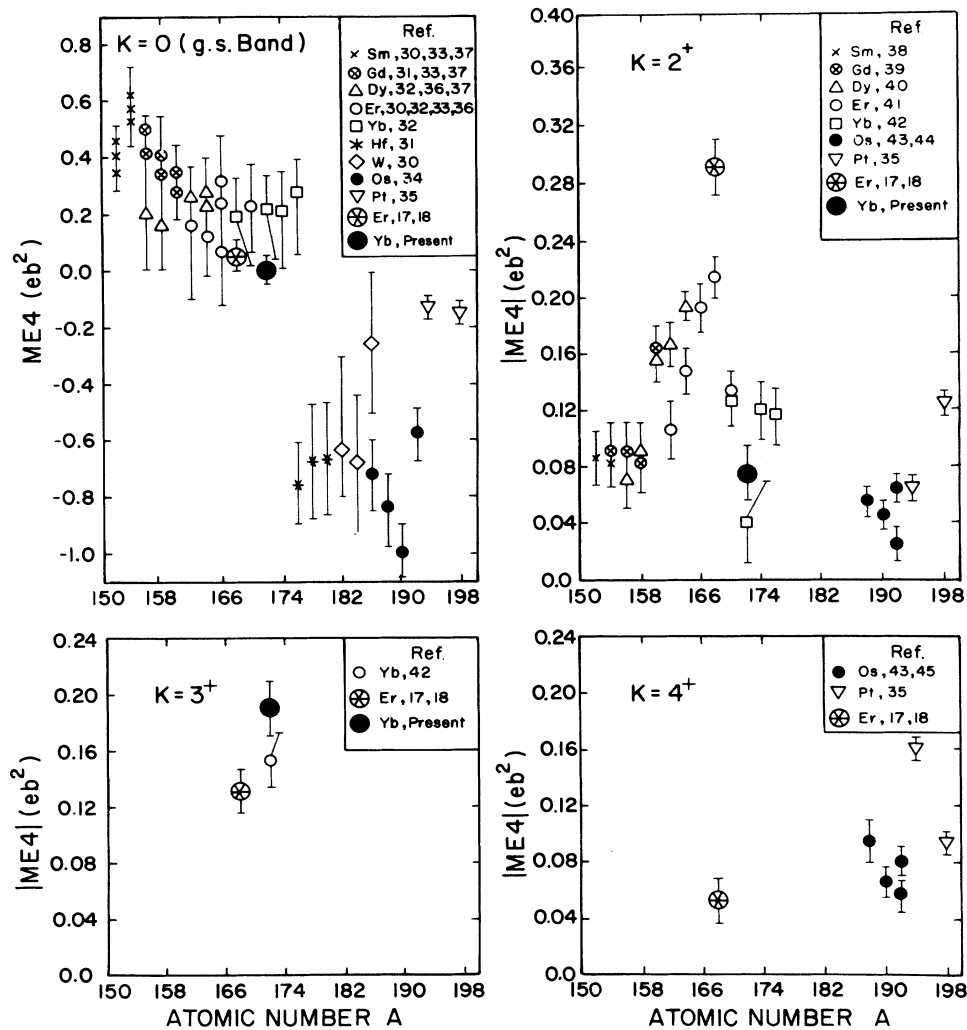


FIG. 9. The experimental matrix element $ME4$ ($0 \rightarrow 4^+$) for transitions from the ground state to 4^+ states of the $K=0$, 2^+ , 3^+ , and 4^+ bands in rare earth nuclei as a function of their mass number.

would be interesting to measure these matrix elements in adjacent mass nuclei. No 4^+ state of the $K=4^+$ band is known in ^{172}Yb while this state in ^{168}Er is excited weakly with a $B(E4)$ value slightly less than one single particle unit.

The summed $E4$ strength to the lowest four 4^+ states is strong in rare earth nuclei, e.g., it is 24 s.p.u. in ^{168}Er and about 10 s.p.u. in ^{172}Yb . The well studied $E4$ transition to the 4^+ member of the $K=0^+$ ground band contributes only 16% of the summed strength for ^{168}Er and 0.5% for ^{172}Yb .

The systematic behavior of the experimental $ME4$ values as a function of mass number (Fig. 9) may be understood qualitatively in terms of the polar cap model of Bertsch.⁴⁸ In this model the transition strengths are related to the shell filling of the valence nucleons. The residual interactions tend to correlate the particles spatially, and the position of the cluster defines a z axis. The added particles are placed in orbitals as close to the z axis as possible. The λ moment of a shell filled to an angle $\cos\theta=\mu$ is given by

$$\left[\frac{2\lambda+1}{4\pi} \right]^{-1/2} \cdot \int_{\mu}^1 Y_{\lambda 0}(\mu) d\mu, \quad (4.3)$$

when the valence particles are filled from the z axis to $\mu = \cos\theta$; i.e., the Fermi surface lies around μ . The transition density from the $K=0$ ground state to the 4^+ states of $K=2^+$, 3^+ , and 4^+ bands can be understood as originating from the superposition of particle-hole excitations within $\Delta\mu$ of the Fermi surface. The λ moments to these bands are proportional to

$$\begin{aligned} & \left[\frac{2\lambda+1}{4\pi} \right]^{-1/2} \cdot \int_{\mu-\Delta\mu}^{\mu+\Delta\mu} Y_{\lambda K}(\mu) d\mu \\ & = \left[\frac{2\lambda+1}{4\pi} \right]^{-1/2} \cdot (2\Delta\mu) Y_{\lambda K}(\mu). \end{aligned} \quad (4.4)$$

Figure 10 shows the qualitative features for the Y_{4K} moments. It is interesting to note that this simple model predicts the mass dependence of the experimental data fairly well. However, a detailed microscopic model is needed to estimate the relative transition strengths. Matsuo⁴⁹ made random-phase approximation (RPA) calculations to understand the observed behavior of $B(E4)$ to the $K=2^+$ γ band in terms of the microscopic structure of the Nilsson single particle orbits near the Fermi surface. His calculations reproduce the mass dependence but underestimate the measured strengths by a factor of 2. Including hexadecupole terms in the residual two-body interaction does not appreciably influence the results of these calculations. Further experimental and theoretical work on the systematics and the model implications of the hexadecupole properties of these nuclei is needed.

V. CONCLUSION

The present study of 36 MeV α scattering displays the collective structure of the low-lying nuclear states in ^{172}Yb . The ground state band is excited up to the 6^+

member, with deformation parameters

$$\begin{aligned} \beta_2 &= +0.21 \pm 0.01, \\ \beta_4 &= -0.028 \pm 0.004, \\ \beta_6 &= 0.0 \pm 0.002. \end{aligned}$$

The isoscalar $E2$ transition strengths to the members of the $K^\pi=2^+$ bands at 1466 and 1608 keV are found to be $0.041 \pm 0.009 e^2 b^2$ (1.4 s.p.u.) and $0.012 \pm 0.003 e^2 b^2$ (0.42 s.p.u.), respectively, weaker than the value ≈ 5 s.p.u. for 821 keV state in the neighboring nucleus ^{168}Er . A notable feature of the present work is the excitation of several 2^+ states at 2184, 2255, 2367, 2465, 2580, 2650, 2738, 2836, 2890, and 2995 keV. The isoscalar transition strengths to these states are found to be larger than the transition strength to the known 2^+ β vibrational state at 1118 keV. The $B(E2)$ strengths found are in reasonable agreement with IBA predictions close to the SU(3) limit.

The 3^- negative parity states at 1222, 1710, 1822, and 2030 keV are excited with a summed isoscalar strength $B(\text{IS}; 0 \rightarrow 3^-) = 0.147 e^2 b^3$ (12 s.p.u.), with an energy centroid at 1832 keV. For the nucleus ^{168}Er the summed strength $= 0.235 e^2 b^3$ (20 s.p.u.) and the centroid is at 1907 keV; in the nearby doubly closed nucleus ^{146}Gd a single 3^- state at 1579 keV yields $B(E3; 0 \rightarrow 3^-) = 0.33 \pm 0.04 e^2 b^3$ (27 s.p.u.). Compared with the theoretical predictions of Neergård and Vogel,²⁷ the results show a marked discrepancy, indicating that these states are not of simple two-quasiparticle RPA character unperturbed or perturbed by Coriolis interaction.

A compilation of the present work with the results of a reanalysis of earlier data from ^{168}Er shows an intriguing

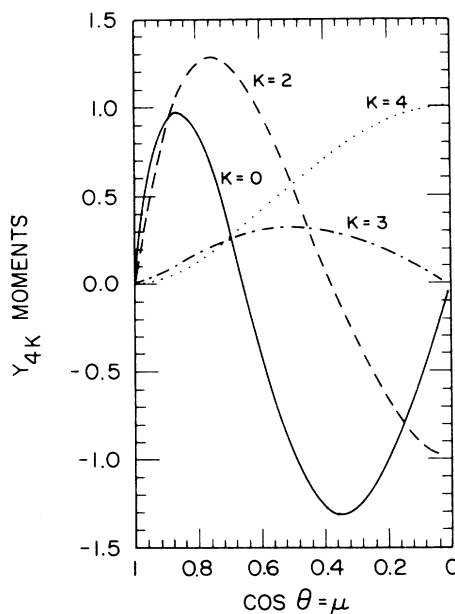


FIG. 10. The intrinsic Y_{4K} moments for $K=0, 2^+, 3^+$, and 4^+ bands according to the Bertsch model of a uniform density covering the polar caps of an aligned nucleus (see text).

ing distribution of the $B(E4)$ values for excitation of the 4^+ members of the lowest $K=2^+$, 3^+ , and 4^+ bands in ^{172}Yb , ^{168}Er , and other strongly deformed rare earth nuclei. Strong $E4$ collective strength has been observed to the $K=2^+$ and 3^+ bands. The $E4$ transition strength to the $K=2^+$ band shows a strong dependence on nuclear species peaking at 16.5 s.p.u. in ^{168}Er and dropping to 1.1 s.p.u. in ^{172}Yb . The 4^+ state of the $K=3^+$ band in ^{168}Er is excited with a collective strength of $0.018 \pm 0.005 e^2 b^4$ (3.5 s.p.u.), while the corresponding state in ^{172}Yb is excited with the strength of $0.036 \pm 0.007 e^2 b^4$ (7 s.p.u.). The summed $E4$ strength in these nuclei exceeds 10 s.p.u. and most of this strength is concentrated in the $K=2^+$ and 3^+ bands. These results are not understood.

The simple picture of the polar cap model by Bertsch⁴⁸ reproduces surprisingly well the observed mass

dependence of the Y_{4K} moments from the ground state to the 4^+ states of $K=2^+$, 3^+ , and 4^+ bands. However, a detailed microscopic theory is needed to explain the relative strengths of these transitions.

ACKNOWLEDGMENTS

The authors wish to thank Dr. D. Burke, Dr. F. T. Baker, Dr. M. N. Harakeh, Dr. R. M. Ronningen, Dr. C. Y. Wu, and Dr. D. Koltun for useful discussions. We also thank the staff of the Nuclear Structure Research Laboratory's operations crew and especially Tom Cormier for help in obtaining an excellent α beam. The support of Mike Satteson during the experiment is appreciated. This research was supported by the National Science Foundation.

*Permanent address: Department of Physics, Panjab University, Chandigarh-160014, India.

¹C. W. Reich, R. C. Greenwood, and R. A. Lokken, Nucl. Phys. **A228**, 365 (1974).

²T. I. Kracikova, S. Davaa, M. Finger, M. I. Fomingka, W. D. Hamilton, P. O. Lipas, E. Hammaren, and P. Toivonen, J. Phys. G **10**, 1115 (1984).

³P. M. Walker, S. R. Faber, W. H. Bentley, R. M. Ronningen, and R. B. Firestone, Nucl. Phys. **A343**, 45 (1980).

⁴J. R. Cresswell, P. D. Forsyth, D. G. E. Martin, and R. C. Morgan, J. Phys. G **7**, 235 (1981).

⁵W. Gelletly, J. R. Larysz, H. G. Börner, R. F. Casten, W. F. Davidson, W. Mampe, K. Schrecken, and D. D. Warner, J. Phys. G **11**, 1055 (1985).

⁶R. C. Greenwood and C. W. Reich, Nucl. Phys. **A252**, 260 (1975).

⁷R. C. Greenwood, C. W. Reich, and S. H. Vegors, Jr., Phys. Lett. **33B**, 213 (1970).

⁸A. Bohr and B. R. Mottelson, *Nuclear Structure* (Benjamin, New York, 1973), Vol. 2,

⁹D. G. Burke and B. Elbek, K. Dan. Vidensk. Selsk. Mat.-Fys. Medd. **36**, No. 6 (1967).

¹⁰V. G. Soloviev, Nucl. Phys. **69**, 1 (1965).

¹¹M. A. Oothoudt and N. M. Hintz, Nucl. Phys. **A213**, 221 (1973).

¹²R. F. Casten, P. Von Brentano, and A. M. I. Haque, Phys. Rev. C **31**, 1991 (1985).

¹³R. O. Sayer, P. H. Stelson, F. K. McGowan, W. T. Milner, and R. L. Robinson, Phys. Rev. C **1**, 1525 (1970); R. O. Sayer, Oak Ridge National Laboratory Report ORNL-TM-2211 (1968).

¹⁴H. J. Wollersheim, W. Wilcke, and T. W. Elze, Phys. Rev. C **11**, 2008 (1975).

¹⁵L. L. Riedinger, E. G. Funk, J. W. Mihelich, G. S. Schilling, A. E. Rains, and R. N. Oehlberg, Phys. Rev. C **20**, 2170 (1979).

¹⁶R. A. O'Neil and D. G. Burke, Nucl. Phys. **A182**, 32 (1972).

¹⁷I. M. Govil and H. W. Fulbright, Bull. Am. Phys. Soc. **29**, 719 (1984).

¹⁸I. M. Govil, H. W. Fulbright, D. Cline, E. Wesolowski, B. Kotlinski, A. Backlin, and K. Grindnev, Phys. Rev. C **33**, 793 (1986).

¹⁹J. Raynal, *Computing as a Language of Physics* (IAEA, Vien-

na, 1972).

²⁰I. M. Govil, H. W. Fulbright, and D. Cline, Bull. Am. Phys. Soc. **31**, 873 (1986).

²¹T. Tamura, Rev. Mod. Phys. **37**, 679 (1965).

²²L. W. Put and M. N. Harekh, Phys. Lett. **119B**, 253 (1982).

²³M. N. Harekh and R. De Leo, Phys. Lett. **117B**, 377 (1982).

²⁴A. M. Bernstein, in *Advances in Nuclear Physics*, edited by M. Baranger and E. Vogt (Plenum, New York, 1969), Vol. 3.

²⁵L. W. Owen and G. R. Satchler, Nucl. Phys. **51**, 15 (1964).

²⁶O. Scholten, program package, "PHINT" IBA-1.

²⁷K. Neergård and P. Vogel, Nucl. Phys. **A145**, 33 (1970).

²⁸I. M. Govil and H. W. Fulbright, Bull. Am. Phys. Soc. **30**, 762 (1985).

²⁹P. Kleinheinz, M. Ogawa, R. Broda, P. J. Daly, D. Haenni, H. Beuscher, and K. Kleinsahn, Z. Phys. A **286**, 27 (1978).

³⁰I. Y. Lee, J. X. Saladin, J. Holden, C. Baktash, C. Bemis, P. H. Stelson, F. K. McGowan, W. T. Milner, J. L. C. Ford, R. L. Robinson, and W. Tuttle, Phys. Rev. C **12**, 1483 (1975).

³¹R. M. Ronningen, J. H. Hamilton, L. Varnell, J. Lange, A. V. Ramayya, G. Garcia-Bermudez, W. Lourens, L. L. Riedinger, F. K. McGowan, P. H. Stelson, R. L. Robinson, and J. L. C. Ford, Phys. Rev. C **16**, 2208 (1977).

³²R. M. Ronningen, R. B. Piercy, J. H. Hamilton, C. F. Maguire, A. V. Ramayya, H. Kawakami, W. K. Dagenhart, and L. L. Riedinger, Phys. Rev. C **16**, 2218 (1977).

³³H. Fischer, D. Kamke, H. J. Kittling, E. Kuhlmann, H. Plicht, and R. Schormann, Phys. Rev. C **15**, 921 (1977).

³⁴F. Todd Baker, T. H. Kruse, W. Hartwig, I. Y. Lee, and J. X. Saladin, Nucl. Phys. **A258**, 43 (1976).

³⁵F. Todd Baker, private communication.

³⁶K. A. Erb, J. E. Holden, I. Y. Lee, J. X. Saladin, and T. K. Saylor, Phys. Rev. Lett. **29**, 1010 (1972).

³⁷A. Shaw and J. S. Greenberg, Phys. Rev. C **10**, 263 (1974).

³⁸E. Veje, B. Elbek, B. Herskind, and M. C. Olsen, Nucl. Phys. **A109**, 385 (1968).

³⁹R. Bloch, B. Elbek, and P. O. Tjom, Nucl. Phys. **A107**, 385 (1968).

⁴⁰T. Grottdal, K. Nybø, and T. Thorsteinsen, and B. Elbek, Nucl. Phys. **A110**, 385 (1968).

⁴¹P. O. Tjom and B. Elbek, Nucl. Phys. **A107**, 385 (1968).

⁴²D. G. Burke and B. Elbek, K. Dan. Vidensk. Selsk. Mat.-Fys. Medd. **36**, No. 6 (1967).

⁴³F. Todd Baker, M. A. Grimm, A. Scott, R. C. Styles, T. H.

- Kruse, K. Jones, and R. Suchanek, Nucl. Phys. **A371**, 68 (1981).
- ⁴⁴D. G. Burke, private communication.
- ⁴⁵D. G. Burke, M. A. M. Shahabuddin and R. N. Boyd, Phys. Lett. **78B**, 48 (1978).
- ⁴⁶W. W. Daehnick, J. D. Childs, and Z. Vrcely, Phys. Rev. C **21**, 2253 (1980).
- ⁴⁷T. Ichihara, H. Sakaguchi, M. Nakamura, M. Yosoi, M. Ieiri, Y. Takeuchi, H. Togawa, T. Tsutsumi, and S. Kobayashi, Phys. Lett. **182B**, 301 (1986).
- ⁴⁸G. F. Bertsch, Phys. Lett. **26B**, 130 (1968).
- ⁴⁹M. Matsuo, Kyoto University Report KUNS-845, 1986.